Toward a coarse-grained model for membranes at interfaces

Author: Abel Hernández Ruiz
*Facultat de Física, Universitat de Barcelona, Diagonal 645, 08028 Barcelona, Spain.**

Advisor: Prof. Giancarlo Franzese

Abstract: The study of water confined at stacked phospholipid bilayers is important to understand basic functions of biological membranes. Within this framework and by means of all-atom molecular dynamics simulations, we analyze the water-membrane and water-water interactions as function of the local distance of water molecules from the membrane. We find that both can be represented as coarse-grained potentials, useful in large-scale simulations.

I. INTRODUCTION

Biological membranes play a key role in preserving vital biochemical processes for living beings. Among all of them, we would emphasize their barrier functions, since they act as cell walls. In this regard, membranes not only keep safe cell contents from its outside, but they also contain embedded proteins that ensure the transport of chemicals through them.

They consist of a lipid bilayer that provides stability. In particular, this project focuses on phospholipid membranes. A characteristic feature of phospholipids is the amphiphilic property, namely they possess both hydrophilic and hydrophobic behaviors. More precisely, they have a phosphate head that is attracted by water and a lipophilic tail that is attracted by lipids (see the red and the gray-colored parts of Fig.(1), respectively). Due to this property, the fact that they form bilayers when surrounded by water is quite clear.

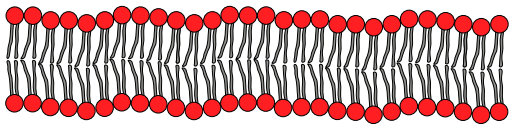

FIG. 1: Sketch of a transversal slice of a phospholipid bilayer.

As shown in the figure above, the two layers are aggregates of phospholipids whose hydrophobic tails attract each other to build the bilayer sheet. This self-assembly process occurs because this orientation leads to a reduction in energy [7].

Moreover, the interface is a soft structure that enables water molecules to partially enter into the membrane, as proven experimentally by means of neutron scattering [5]. The antiparallel orientation of both layers and the flexibility of the whole ensemble relies on the negligible rate of lipids transverse diffusion against the lateral one [7], so that a lipid flip-flop is rather unlikely.

Here we consider a lamellar structure of several phospholipid bilayers separated by bulk water. At ambient conditions thermal fluctuations are such that the water density profile near the membrane interface is smeared out as a continuous function, going from zero density inside the membrane to bulk density away from the membrane, over a distance of the order of 1 nm [10]. Nevertheless, a careful analysis based on the definition of an instantaneous local distance of water molecules with respect to the head of the nearest phospholipid reveals a structure of the density profile with a clear hydration shell and with a complex dynamics [2]. In particular, we can distinguish an almost immobile 'inner' water inside the membrane, a very slow 'bound' hydration water at the interface with the membrane and a slow 'unbound' water separating the bound water from the bulk [1].

In this work we will analyze in detail the different components of the water-membrane and water-water interactions as function of the instantaneous local distance to find connections between their cumulative interaction with the different hydration layers. This study will provide insight into how to develop coarse-grained models of these interactions, a relevant result for large-scale simulations of biological systems.

II. METHODS

We consider 128 dimyristoylphosphatidylcholine (DMPC) lipids forming a bilayer, surrounded by 7040 water molecules, corresponding to a hydration level $\omega = 55$, with periodic boundary conditions, as in Fig.(2). We analyze $f = 1000$ frames of 50 ns long Molecular Dynamics trajectories at ambient conditions, 303 K and 1 atm, that have been simulated with the NAMD 2.9 free-software, adopting for DMPC and water interactions the CHARMM36 (Chemistry at HARvard Molecular Mechanics) force field parameters with TIP3P water, a combination that is able to reproduce the area per lipid in excellent agreement with experimental data. Further details for the simulations are availabe in Ref. [1]. Trajectories are analyzed with the open-source Visual Molecular Dynamics (VMD) software that, together with in-house scripts, allows us to visualize and calculate all the quantities reported in this work.

Each TIP3P water molecule is rigid with 3 point charges distributed in a way to reproduce at the best

*Electronic address: abel.ahr@gmail.com

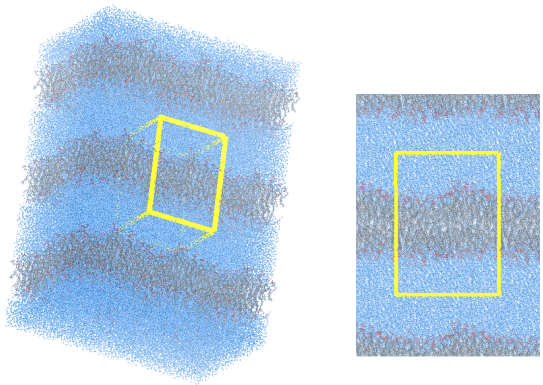

FIG. 2: Snapshot of the simulation box (yellow rectangular parallelepipid) with periodic boundary conditions: water molecules and phospholipids are represented in blue and gray, respectively.

the water dipole moment, its energies and some of its thermodynamics properties. Likewise, the DMPC lipids have 118 point charges: 1 nitrogen of the choline group, 1 phosphorous of the phosphate, 8 oxygens (1 of the choline, 4 of the phosphate and 3 of the glycerol), 36 carbons and 72 hydrogens [8, 9].

The long-range Coulomb potential energy of the interaction between atoms i and j at time t is

$$E_{ij}^{\text{Coulomb}}(t) = \frac{q_i q_j}{4\pi\epsilon_0 r_{ij}(t)}, \tag{1}$$

where ϵ_0 is the vacuum permittivity, q_i and q_j are the point charges of atoms i and j, respectively, and $r_{ij(t)}$ is the interatomic distance. The long-range electrostatic forces are computed using the particle mesh Ewald method with a grid space of ≈ 1 Å and are updated every 2 fs [2].

Since the simulations are performed at constant temperature and pressure, the simulation box dimensions depend on the selected frame and thus we can denote them by $L_x(t)$, $L_y(t)$ and $L_z(t)$, where $t \in \{1, 2, 3, \ldots, 1000\}$ is the frame index. Accordingly, we compute the Euclidean distance $r_{ij}(t)$ between two points, say $(x_i(t), y_i(t), z_i(t))$ and $(x_j(t), y_j(t), z_j(t))$, as

$$\sqrt{\sum_{c\in\{x,y,z\}} \left(\min\{|c_i(t) - c_j(t)|, L_c(t) - |c_i(t) - c_j(t)|\}\right)^2}. \tag{2}$$

Furthermore, the force field includes van der Waals interactions between each pair of atoms to reproduce the medium-range dispersive attractive forces and the short-range repulsive forces due to the Pauli's exclusion principle for the orbital electrons. These interactions for each pair of atoms i and j at time t are represented with the Lennard-Jones (LJ) potential

$$E_{ij}^{\text{LJ}}(t) = \varepsilon_{ij}\left[\left(\frac{R_{ij,\min}}{r_{ij}(t)}\right)^{12} - 2\left(\frac{R_{ij,\min}}{r_{ij}(t)}\right)^{6}\right], \tag{3}$$

where ε_{ij} is the attractive energy and $R_{ij,\min}$ is the distance at which the potential reaches its minimum, with $\varepsilon_{ij} = \sqrt{\varepsilon_i \varepsilon_j}$ and $R_{ij,\min} = (R_{i,\min} + R_{j,\min})/2$ for atoms i and j of different species [6]. The van der Waals interactions have a cutoff at 12 Å with a smooth switching function starting at 10 Å [2].

Following Pandit *et al.* [11], we assign at each time t and to each water molecule i the instantaneous local distance $\xi_i(t)$ from the membrane defined as follows.

1. Perform a two-dimensional Voronoi tessellation of the average plane of the membrane (the xy-plane) using the phosphorous and nitrogen atoms of the phospholipid heads as centers of the Voronoi cells.
2. Project the molecule i onto the xy-plane and assign to it the corresponding Voronoi cell.
3. Let $\overline{\xi}$ be the distance along the z-axis between i and the seed of its Voronoi cell. If i is inside the membrane, then $\xi_i(t) := -\overline{\xi}$. Otherwise, $\xi_i(t) := \overline{\xi}$.

We assign the value ξ with a resolution of $\Delta_\xi = 0.2$ Å to all water molecules.

III. RESULTS

The water distribution is given by the average molecular number density,

$$n(\xi) := f^{-1}\sum_{t=1}^{f}(L_x(t)L_y(t)\Delta_\xi)^{-1}\sum_{i=1}^{n_w}\delta(\xi, \xi_i(t)), \tag{4}$$

where $\delta(\cdot,\cdot)$ is the Kronecker delta and n_w is the number of molecules within the simulation box (7040 in our case).

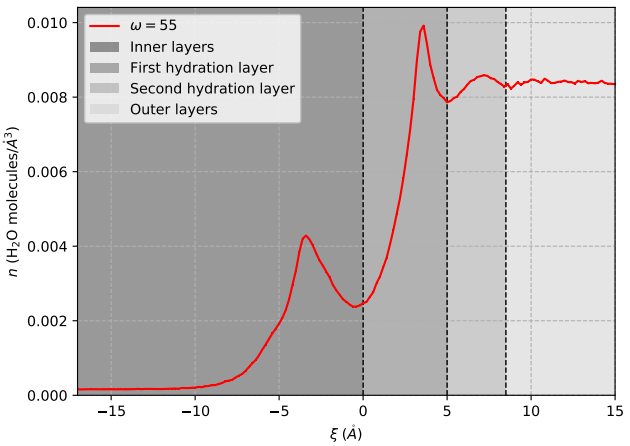

FIG. 3: Average water molecular number density with a resolution of $\Delta_\xi = 0.2$ Å. Negative values of ξ correspond to water inside the membrane.

Fig.(3) shows the penetration of water into the headgroups region $\xi < 0$ and two hydration layers for $\xi > 0$. The local minima of the density profile show the first

hydration layer for $0 < \xi < 5$ Å and the second for 5 Å $< \xi \lessapprox 8.5$ Å, close to the 1 nm that is often invoked as the length-scale below which water molecular details are dominating its structure and dynamics [3, 4].

Now, we introduce in a general manner an analytic formula of such total energies in terms of hypothetical interactions $E_{ij}(t)$ between a water molecule $i \in \{1, 2, 3, \ldots, n_w\}$ and any other atom $j \in \{1, 2, 3, \ldots, a\}$.

Let $Q(\xi; t)$ be the last summation of Eq.(4). If $Q(\xi; t) \neq 0$, we define the average energy of a water molecule of the frame t with relative coordinate ξ as

$$\tilde{E}(\xi; t) \coloneqq \left[\sum_{i=1}^{n_w} \delta(\xi, \xi_i(t)) \sum_{i=1}^{a} E_{ij}(t)\right] (Q(\xi; t))^{-1} \quad (5)$$

and, otherwise, we set $\tilde{E}(\xi; t) \coloneqq 0$. Correspondingly, we consider the following expression for the average energy of a water molecule as a function of ξ

$$E(\xi) \coloneqq \left(\sum_{t=1}^{f} \tilde{E}(\xi; t)\right) \left[f - \sum_{t=1}^{f} \delta(0, Q(\xi; t))\right]^{-1} . \quad (6)$$

Fig.(4) shows our calculations for the average of the total interaction energy $E^{\text{Coulomb}} + E^{\text{LJ}}$ of water molecules at instantaneous local distance ξ from the membrane.

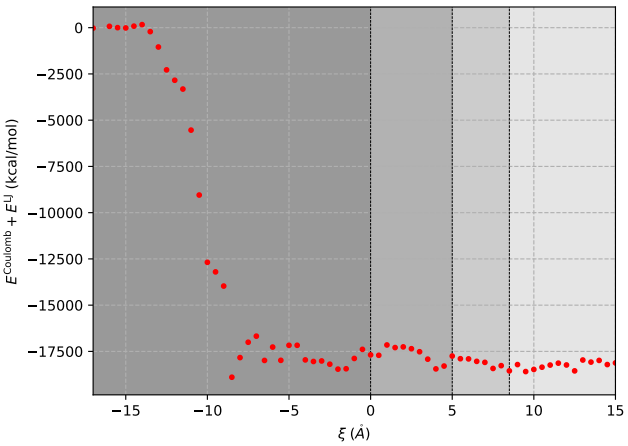

FIG. 4: Average total potential energy of water molecules at instantaneous local distance ξ from the membrane, with a resolution of $\Delta_\xi = 0.5$ Å. Gray regions are defined as in Fig.(3).

At first glance, the total interaction energy of water molecules seems almost independent on the instantaneous local distance ξ for $\xi > -10$ Å, including the region inside the membrane. This result apparently suggests that water could freely penetrate within the membrane. However, these calculations for the potential energy do not account for the entropy component of the water Gibbs free energy as function of ξ. Recent calculations [1] show a large slowing down of the dynamics of water approaching and penetrating the membrane. As a consequence, the number of visited configurations per unit of time (entropy production) is reduced, implying a large entropy decrease for water near and inside the membrane.

To better understand the origin of our results in Fig.(4), we calculate each of the components of the total potential energy: water-lipids and water-water LJ potential energy; water-lipids and water-water electrostatic potential energy (see Fig.(5)).

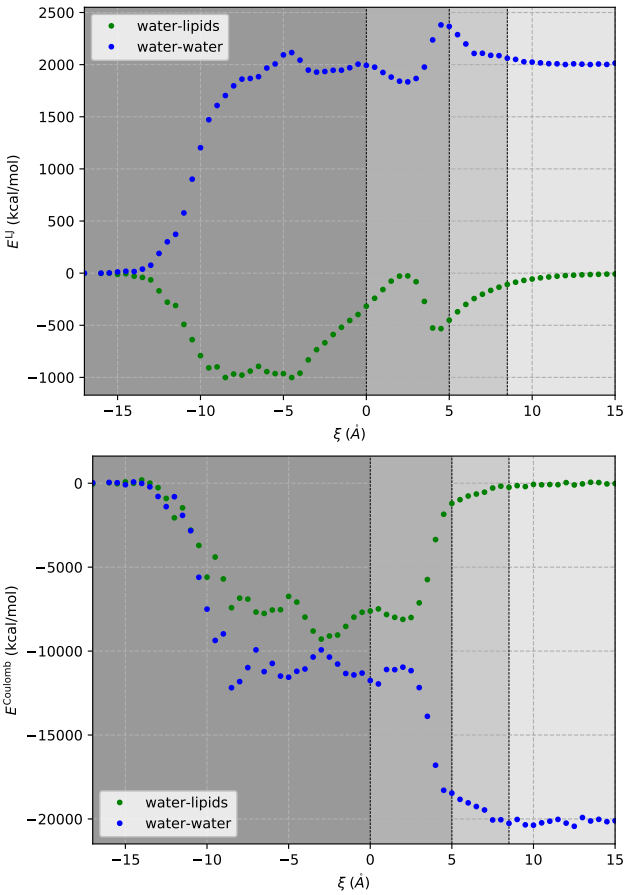

FIG. 5: Water-lipids (green points) and water-water (blue points) average LJ (upper panel) and electrostatic contributions (lower panel) to the potential energy of water molecules at instantaneous local distance ξ from the membrane, with a resolution of $\Delta_\xi = 0.5$ Å. Gray regions are defined as in Fig.(3).

We find that water-water LJ interactions are repulsive, i.e. water molecules are held by their strong electrostatic interactions (giving rise to the hydrogen bonds) at a relative distance that is shorter than their van der Waals diameter, while LJ interactions with the lipids are attractive. However, the LJ interactions are at least one order of magnitude weaker than both the water-water and water-lipids Coulomb interactions. The water-water Coulomb interactions are dominant outside the membrane, while inside the membrane they are of the same order of magnitude as the water-lipids electrostatic interactions, consistent with the relatively high density of

water hydrating the lipid headgroups at $\xi < 0$. The large difference in order of magnitude between van der Waals and electrostatic contributions to the potential energy seems to suggest that the first plays a minor role in the energy balance of hydration water. Nevertheless, by calculating the total (repulsive) LJ contribution (see Fig.(6)) it is possible to observe that there is a clear correlation between its minima and the maxima in the water density profile Fig.(3). Therefore, the local minima in the LJ interaction energy seem to have a relevant role in determining the hydration water density profile.

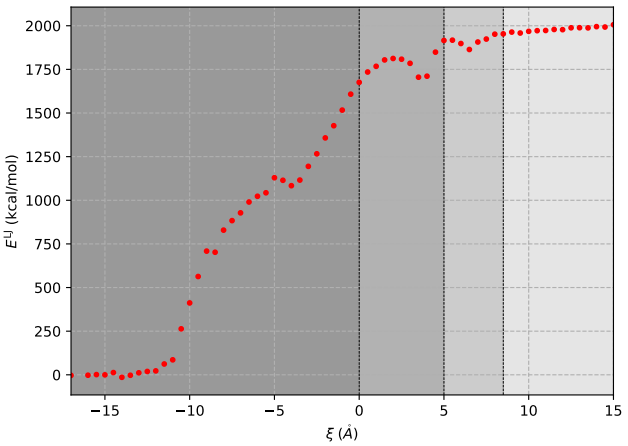

FIG. 6: The sum of the water-water and water-lipids LJ components, shown in the upper panel of Fig.(5) with a resolution of $\Delta_\xi = 0.5$ Å, has three minima that correlate well with the three maxima in the three darkest regions of Fig.(3).

Finally, we show the total water-lipids interaction energy (see Fig.(7)).

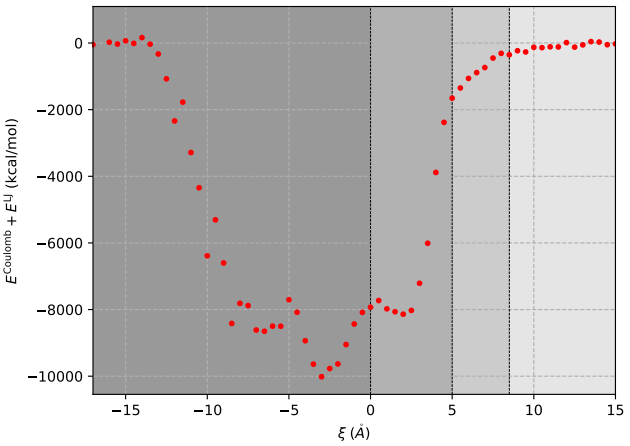

FIG. 7: Average lipids contribution to the total water potential energy with a resolution of $\Delta_\xi = 0.5$ Å.

We observe that this overall interaction has four distinctive behaviors with respect to the membrane: it is deeply attractive with a minimum at ≈ -4 Å inside the membrane, where the phospholipid headgroups are approximately located; it is attractive for water in the first hydration shell with a minimum at ≈ 2.5 Å outside the membrane; it has a crossover to a less attractive region with no minimum for water in the second hydration shell; it has approximately zero interaction with water molecules at an instantaneous local distance larger than ≈ 1 nm.

IV. CONCLUSIONS

We analyze MD simulations of DMPC phospholipid bilayers and hydration water. We calculate the water density profile and the water-lipids and water-water interaction components as functions of the instantaneous local distance of the water molecules from the lipid headgroups N and P atoms. The local distance reveals that hydration water forms layers (two at our hydration level) expanding up to ≈ 1 nm and that it penetrates into the membrane for ≈ 0.5 nm, confirming recent calculations at different hydration levels [1, 2].

We find that the total potential energy of hydration water is dominated by the electrostatic contributions, that overcome by one order of magnitude the van der Waals interactions. The total water potential energy does not change strongly when water penetrates the membrane, suggesting that the entropy contribution to the free energy plays a major role in ruling the water density profile.

Nevertheless, the entropy is expected to be smaller for the bound water in the first hydration layer with respect to the bulk and even smaller for the inner water in the membrane. This suggests that the entropy contribution to the Gibbs free energy should favor water away from the membrane. This observation is in apparent contrast with the increased density profile of water near the membrane. Yet, the density profile is inversely proportional to the exponential of the Gibbs free energy variations (in units of the thermal energy k_BT, where k_B the Boltzmann constant and T the absolute temperature). Therefore, our calculations show that the small minima observed in Fig.(4), once combined with the entropy variation, are enough to give the large changes in density profile in Fig.(3).

Further analysis shows that the water-water van der Waals interactions are always repulsive, while the water-lipids van der Waals interactions are weaker and attractive. The total van der Waals potential energy is, hence, repulsive, but has local minima that correlate well with the peaks of the water density profile. Thus, these minima seem to give a relevant contribute to the total water potential energy, despite their small values.

Finally, we are able to characterize the overall water interactions with lipids as function of the local distance ξ, finding four distinctive regions within our resolution $\Delta_\xi = 0.5$ Å. Our calculations for higher resolution, $\Delta_\xi = 0.2$ Å, show that to reduce the noise we should largely increase the statistics of our sampling (see Appendix). This result could be relevant for developing

a coarse-grained interaction model of water with membranes useful in large-scale simulations of biological systems, within a multi-scale approach.

Acknowledgments

I would like to express my gratitude to Dr. Carles Calero and Prof. Giancarlo Franzese for their continuous help and guidance all along this research. Finally, I wish to mention some special people in my native languages. A mi hermana, mi madre y mi padre; qué suerte la mía, os quiero. Júlia, mai oblidaré les teves classes, els teus consells i el treball de recerca que vam fer junts; gràcies per fer-me estimar la física.

V. APPENDIX

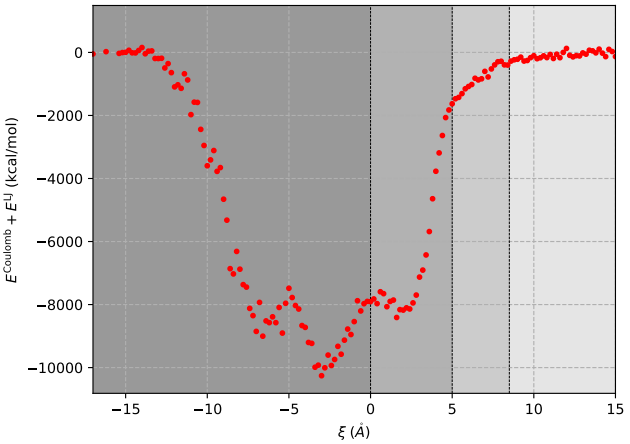

FIG. 8: Average lipids contribution to the total water potential energy with a resolution of $\Delta_\xi = 0.2$ Å. The noise increases compared to Fig.(7), probably due to poor sample statistics.

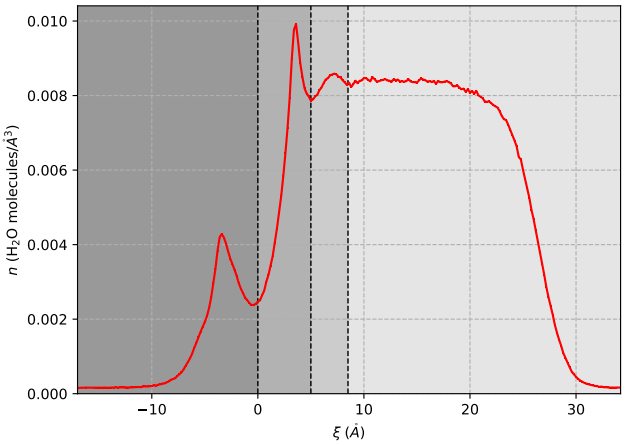

FIG. 9: Unsymmetrized water density profile at large local distance from the membrane shows that there are only a few water molecules for $\xi > 15$, that can be occasionally found due to membrane fluctuations.

[1] Calero, C., Franzese, G. Membranes with different hydration levels: The interface between bound and unbound hydration water. *Journal of Molecular Liquids* **2019**, *273*, 488.

[2] Calero, C., Stanley, H., Franzese, G. Structural Interpretation of the Large Slowdown of Water Dynamics at Stacked Phospholipid Membranes for Decreasing Hydration Level: All-Atom Molecular Dynamics. *Materials* **2016**, *9*, 319.

[3] Chandler, D. Interfaces and the driving force of hydrophobic assembly *Nature* **2005**, *437*, 640-7, and references therein.

[4] de los Santos, F., Franzese, G. Relations between the diffusion anomaly and cooperative rearranging regions in a hydrophobically nanoconfined water monolayer. *Physical Review E* **2012**, *85*, 010602.

[5] Fitter, J., Lechner, R.E., Dencher, N.A. Interactions of hydration water and biological membranes studied by neutron scattering. *J. Phys. Chem. B* **1999**, *103*, 8036-8050.

[6] Fyta, M. (2016). *Computational Approaches in Physics.* Morgan & Claypool Publishers.

[7] Hamley, I.W. (2007) *Introduction to Soft Matter: Synthetic and Biological Self-Assembling Materials.*

[8] Klauda, J.B., Venable, R.M., Freites, J.A., O'Connor, J.W., Tobias, D.J., Mondragon-Ramirez, C., Vorobyov, L., MacKerell, A.D., Pastor, R.W. Update of the CHARMM all-atom additive force field for lipids: Validation on six lipid types. *J. Phys. Chem. B* **2010**, *114*, 7830-7843.

[9] Lim, J.B., Rogaski, B., Klauda, J.B. Update of the cholesterol force field parameters in CHARMM. *J. Phys. Chem. B* **2012**, *116*, 203-210.

[10] Martelli, F., Ko, H.Y., Calero, C., Franzese, G. Structural properties of water confined by phospholipid membranes. *Frontiers of Physics* **2017**, *13*, 136801.

[11] Pandit, S.A., Bostick, D., Berkowitz, M.L. An algorithm to describe molecular scale rugged surfaces and its application to the study of a water/lipid bilayer interface. *J. Chem. Phys.* **2003**, *119*, 2199-2205.